

## THE FLARE OF 1989 SEPTEMBER 9, 09:09 UT: DOES CORONAL LOOP COLLISION INITIATE EFFICIENT GAMMA-RAY EMISSION?

H. AURASS

Astrophysikalisches Institut Potsdam, Observatorium für Solare Radioastronomie, 14552 Tremsdorf, Germany

A. HOFMANN

Astrophysikalisches Institut Potsdam, Sonnenobservatorium Einsteinurm, 14473 Potsdam, Telegrafenberg, Germany

AND

E. RIEGER

Max-Planck-Institut für Extraterrestrische Physik, 85748 Garching, Germany

Received 1993 February 22; accepted 1993 June 25

### ABSTRACT

Vector magnetogram data and  $H\alpha$  pictures together with data published by Chupp et al. lead us to conjecture that in the presented case a contact between the rising two-ribbon flare current sheet and a coronal loop connecting two nearby plage regions initiates efficient high-energy  $\gamma$ -ray emission.

*Subject headings:* Sun: corona — Sun: flares — Sun: X-rays, gamma rays

### 1. INTRODUCTION

One of the key problems of flare physics is the energy release and particle acceleration process. A successful confrontation of theory and data demands a detailed knowledge of the magnetic field topology of the flaring solar active region (vector magnetograms), information about the time evolution of the chromospheric reaction to the coronal energy input (flare ribbon geometry from  $H\alpha$  images with high time resolution), and monitoring of the accelerated particle dynamics by their coronal radio signature in time and spectrum with image resolution. Additional hard X-ray and  $\gamma$ -ray data allow for the recognition of flares, respectively, flare phases with especially efficient particle acceleration and with a significant amount of protons in the accelerated particle ensemble (e.g., Ramaty & Murphy 1987; Rieger 1989; Chupp 1990). In this paper we deal with a vector magnetogram of solar active region NOAA 5680 which was recorded immediately before the (1B, X1) flare on 1989 September 9, 09:09–09:25 UT. This flare attracted our attention because of a brief (20 s) high-energy emission pulse (electron bremsstrahlung up to 40 MeV; nuclear line emission 1–7 MeV; see Fig. 1). Chupp et al. (1993) have additionally published high-resolution  $H\alpha$  and radio data of this flare. We find that a contact between the developing two-ribbon flare system and an independent coronal loop rooted in two plage regions acts as a trigger of enhanced high-energy particle creation.

### 2. OBSERVATIONS

#### 2.1. Magnetic Field Structures and Active Region Development

Figure 2 gives an overview of the magnetic field topology around AR 5680. The flare to evolve (it started about 20 minutes past the recording of this image) is located to the north of the big southern polarity leading spot ( $S_0$ ). There we find a

nearly circular north polarity structure ( $N_1$ ) being the follower part of a bipolar region of smaller scale. In white light this structure consists of a pore accompanied by a nonregular penumbra stretched toward the small leader part  $S_1$ . During the period of our magnetographic observations from September 8 until September 13 the structure  $N_1$  moves eastward. The probable driver of this long-term movement is the development in AR 5683 (NEF in Fig. 2) where new flux was emerging rapidly to the northwest of spot  $S_0$  pushing aside the preexisting (smaller scale) flux. On 1989 September 9 the first flare from this active region (1B, M1.4; 05:29–05:50 UT observed in  $H\alpha$  at Athens; *SMM* was in spacecraft night) is characterized by  $H\alpha$  flare ribbons exactly at the sites of largest field gradients designated by A and B (Fig. 3, top). Three hours later postflare loops (PFL in Fig. 2) of this event were observed. Before the 09:09 UT flare the active region filament ( $F$  in Fig. 2) is nearly circularly surrounding the north polarity magnetic intrusion.

#### 2.2. The 09:09 UT Flare

Consequently we see at 09:09–09:23 UT the  $H\alpha$  flare having a circular ribbon  $B$  (Fig. 3, bottom) around a dotlike ribbon  $A$ . As evident from Figure 1, with a time delay of about 50 s, an additional energy release occurred which according to Chupp et al. (1993) was accompanied by the simultaneous appearance of two  $H\alpha$  brightenings  $C$  and  $D$  (Fig. 3, bottom) at the former plage regions between 09:10 and 09:11 UT. The southward positioned region  $C$  corresponds with the newly emerging flux region (NEF in Fig. 2). The mutual brightening of  $C$  and  $D$  in the wings of  $H\alpha$  indicates the magnetic connection between both plage regions by an activated loop with large coronal height extension—at least  $81 \times 10^6$  m top height by a semicircular approach corresponding with a top plasma frequency of 320 MHz in a generally accepted Newkirk active region density model. Possibly the noise storm source noted by Chupp et al. (1993) in the preflare phase is situated in this

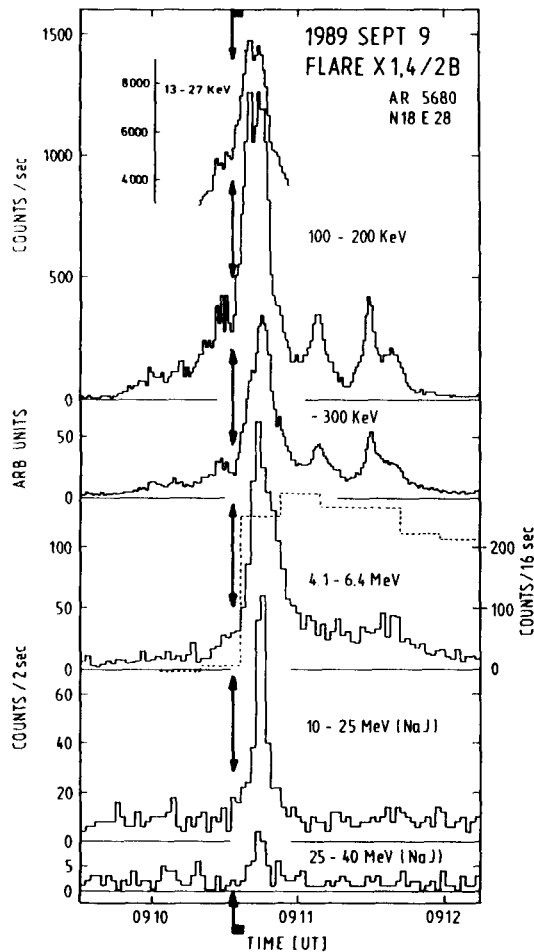


FIG. 1.—The 1989 September 9 flare as seen in X-rays and  $\gamma$ -rays by *SMM* (Rieger 1991). A short pulse of high-energy emission is observed roughly 50 s after the onset in hard X-rays. It consists of electron bremsstrahlung up to 40 MeV and nuclear line emission between 1 and 7 MeV. The dashed line denotes the intensity of the 2.2 MeV neutron capture line (right-hand scale). The arrows and the thick bars mark onset and duration of the spatially and spectrally isolated radio source at 327 MHz reported by Chupp et al. (1993); see the discussion in § 3.

loop, because the active region loops connecting *A* and *B* (Fig. 3) do not reach such heights. The association of the “secondary brightenings” at *C* and *D* with the main impulsive feature in the  $\gamma$ -ray data of Figure 1 is somewhat surprising. In Table 1 we summarize our findings.

### 3. DISCUSSION

#### 3.1. General Remarks

Until now no special topological features have been reported in cases where magnetic field data were available for  $\gamma$ -ray flares. Hagyard & Smith (1990) compared vector magnetograms of five flares and concluded that in connection with  $\gamma$ -ray flares the field is sheared over a longer length of the neutral line. In the present case we noticed two remarkable features (Fig. 3, bottom):

1. The circular flaring around the intruded plage feature *A*.
2. The “secondary brightenings” (term used by Herant, Golub, & Neidig 1989).

Circular flares are rare (e.g., Akasofu 1984) but not known to be related with powerful energy release. The appearance of “secondary brightenings” during flares is frequent (e.g., Tang 1985; Machado et al. 1988; Herant et al. 1989). It is usually interpreted as a signature of the spreading of the flare energy release into further bipolar parts of the active region (Machado et al. 1988) by contacts between the already flaring and earlier independent magnetic loops. This process is schematically depicted by Herant et al. (1989) who assume that the newly involved loop system passes through the preexisting main two-ribbon flare current sheet. It is interesting to note that Wuelser, Canfield, & Rieger (1990) identify in  $H\alpha$  data a “secondary component within the same active region but well apart from the main flare ribbons” as simultaneously acting with the high-energy  $\gamma$ -ray event for another flare.

#### 3.2. Loop Collision in AR 5680?

In our case we know from the data presented by Chupp et al. (1993) that the incorporation of the separate structure *C-D* into the already ongoing main flare initiates a huge growth of high-energy particle acceleration. Note especially that the *C-D* brightening in  $H\alpha$  is associated with the simultaneous appearance of a new spatially isolated radio burst component between the main flare source at *A-B* and the preflare noise storm source probably associated with the *C-D* loop. This source has a narrow-band spectrum ( $\Delta f/f < 0.3$ ) and was noticed at the 327 MHz image taken with the Nançay radio heliograph only, quite in contrast with the main radio flare from region *A-B* visible at all the five Nançay observing frequencies in the range 150–450 MHz (see Chupp et al. 1993). Remember that we have guessed a probable top height of 81,000 km for the *C-D* connecting loop corresponding with the 320 MHz plasma level! Thus the narrow-band decimeter emission (onset and duration are shown by arrows and a thick bar in Fig. 1 as found by Chupp et al. 1993) seems to come directly from the assumed contact region between the rising two-ribbon flare current sheet and the *C-D* coronal loop. In Figure 4 we draw schematically the situation in the corona above AR 5680.  $H\alpha$  flare ribbons and brightenings are shown in a perspective view from the south (compare with Fig. 3, bottom). Above the magnetic field lines connecting the flare ribbons “*A-B*” we draw (idealized) the current sheet CS according to the two-ribbon flare geometry with the filament *F* at the top, assuming an inverse-polarity configuration (Leroy 1989). The currents in the two-ribbon flare system and in the interconnecting loop *C-D* are contradirected and should attract each other. We claim that the contact between the flaring current sheet and the coronal loop results in the short spectrally and spatially isolated decimetric radio pulse. Notice that the decimeter radio range is frequently identified as enclosing the coronal primary energy release site (e.g., Zaitsev & Stepanov 1983; Benz 1985). Aurass & Kliem (1992) found in decimeter radio fine structures of narrow-band decimeter continua typical signatures of dynamic current sheet evolution.

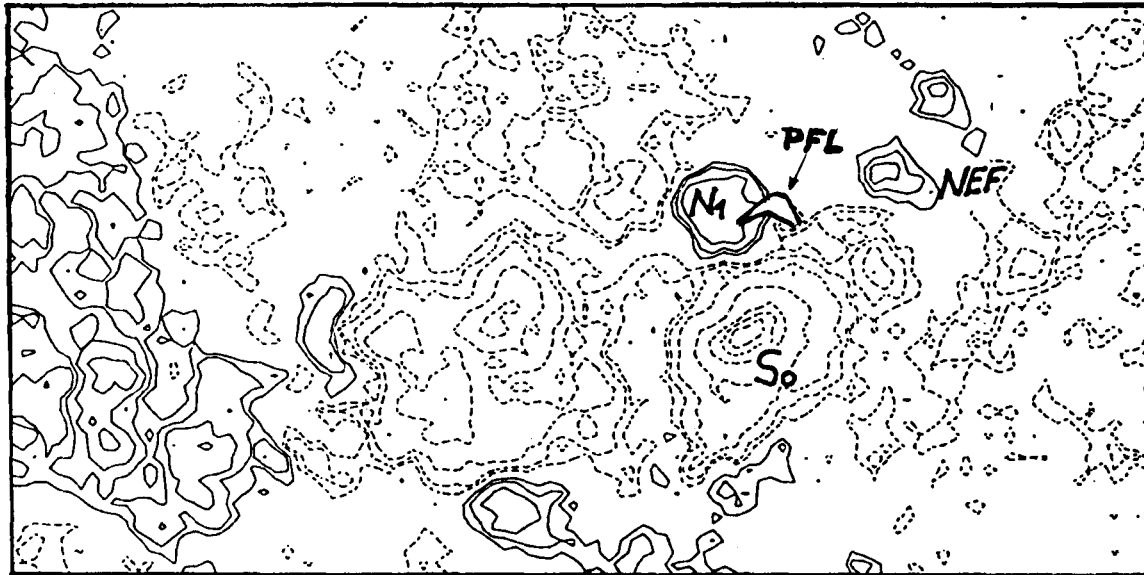
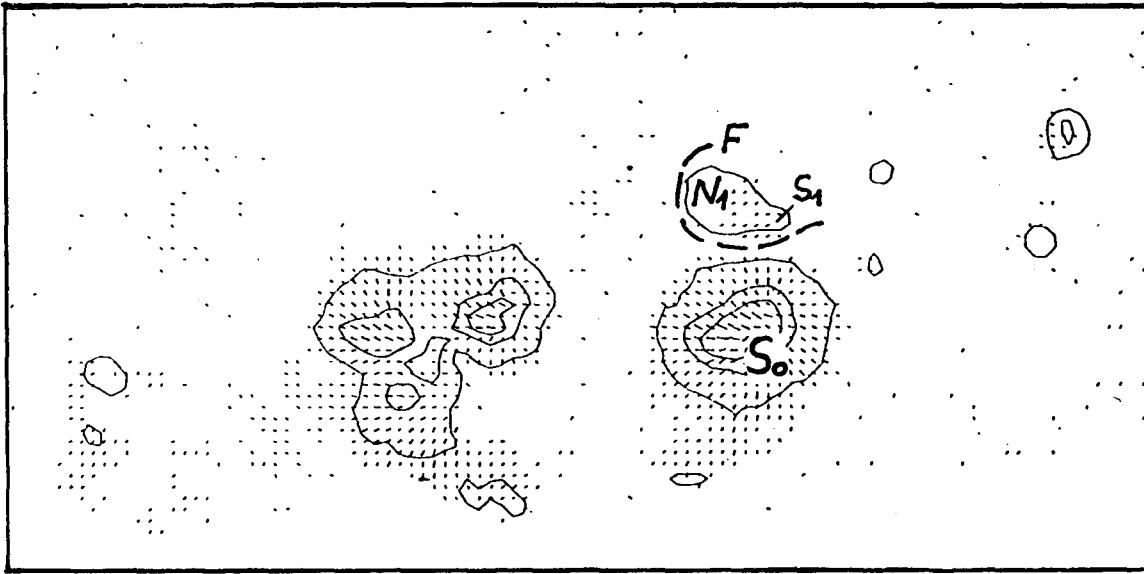


FIG. 2.—The Potsdam magnetogram ( $5250.2 \text{ \AA}$  blue wing) of 1989 September 9 taken between 07:37 and 08:44 UT. The upper-left-hand corner of the picture ( $276'' \times 138''$ ) is at N24 E41; north is top, east is left. *Top*: brightness contours and azimuth of the transversal field component. Isoline levels (quiet Sun = 1000): 850, 550, 300.  $S_0$ : the large leading south polarity spot;  $N_1$ : nearly circular north polarity structure being the follower of the small-scale bipolar region ( $S_1$ ,  $N_1$ ) which in white light is a pore accompanied by a nonregularly stretched penumbra;  $F$ : a nearly circular active region filament. *Bottom*: the corresponding longitudinal field magnetogram. Isoline levels 40, 80, 160, . . . , 1280. *Solid*: north; *dashed*: south. *PFL*: postflare loops from an earlier flare, visible on a Potsdam  $H\alpha$  image; *NEF*: region of newly emerging north polarity magnetic flux. A south polarity NEF region is positioned about 81,000 km to the northwest and was out of the actual field of view of the magnetograph.

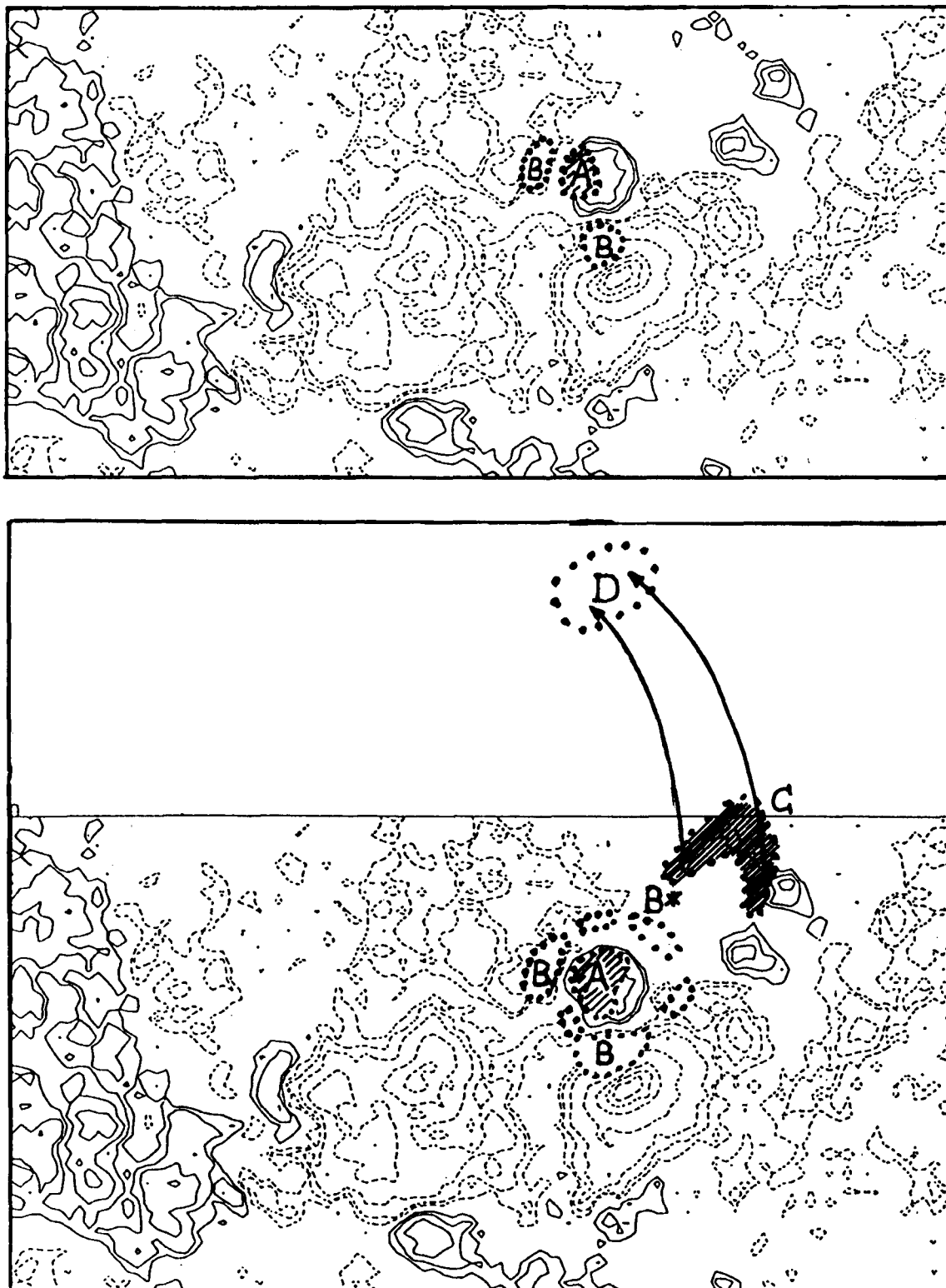


FIG. 3.—Same as bottom panel of Fig. 2 with flare ribbons of  $H\alpha$  flares taken from images kindly provided by T. Prokakis, Athens. *Top*: the (1B, M1.4)  $H\alpha$  flare at 05:29–05:50 UT. Ribbons are designated by “A” and “B” with regard to the different magnetic polarity of the photospheric field. *Bottom*: the flare ribbons and  $H\alpha$  brightenings of the (1B, X1) flare 09:09–09:25 UT. “A” is a nearly dotlike ribbon above the north polarity intruded pore, surrounded by the “B” circular ribbon. A large-scale coronal loop interconnects regions “C” and “D”. It organizes their simultaneous “secondary brightening in  $H\alpha$ ” in the same minute in which the high-energy emission is noticed according to Chupp et al. (1993).

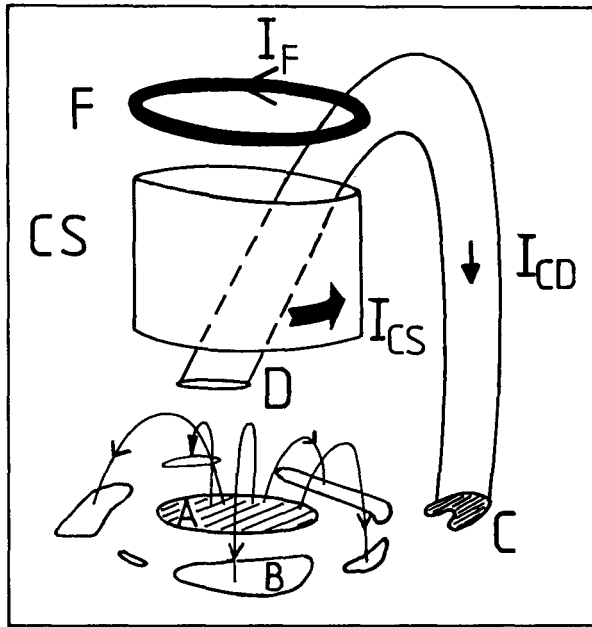


FIG. 4.—Sketch of a scenario to explain the observations. For explanation see § 3.

After this pulse which slightly precedes the main  $\gamma$ -ray emission (see Fig. 1) the already flaring broad-band radio source is enhanced in morphological correspondence with the  $\gamma$ -ray and hard X-ray light curves shown by Chupp et al. (1993). Probably the contact of the loop  $C$ - $D$  with the dynamic current

TABLE I  
SUMMARY OF OBSERVATIONS

Time Interval (UT)	Fact
09:09–09:23 .....	Primary, circular ribbon $H\alpha$ , flare
09:10–09:11 .....	Secondary $H\alpha$ brightening (loop height deduced from geometry implies a 320 MHz radio emission frequency)
$\approx$ 09:10:30 .....	Narrow-band radio emission at 327 MHz observed as located between primary and secondary brightenings
$\approx$ 09:10:40 .....	$\gamma$ -ray maximum (Fig. 1)

sheet leads (in an unknown manner) to an extreme enhancement of its particle acceleration efficiency.

From the experience of two cases we propose to check if such an interaction of the two-ribbon flare current sheet and an additional magnetic loop is a necessary condition for  $\gamma$ -ray-efficient energy release.

The authors are very grateful to T. Prokakis, National Observatory of Athens, Astronomical Institute of Athens University, for his kind presentation of two  $H\alpha$  images of AR 5680. Further, we thank B. Kalman of the Debrecen Solar Observatory for his comments concerning motions of sunspots in the same active region, and to an anonymous referee for very helpful suggestions.

#### REFERENCES

- Akasofu, S. I. 1984, *Planet. Space Sci.*, 32, 1469  
 Aurass, H., & Kliem, B. 1992, *Sol. Phys.*, 141, 371  
 Benz, A. 1985, *Sol. Phys.*, 96, 357  
 Chupp, E. L. 1990, *Science*, 250, 229  
 Chupp, E. L., Trotter, G., Marschhäuser, H., Pick, M., Soru-Escout, I., Rieger, E., & Dunphy, P. P. 1993, *A&A*, 275, 602  
 Hagyard, M. J., & Smith, J. B., Jr. 1990, *ApJS*, 73, 159  
 Herant, M., Golub, L., & Neidig, D. F. 1989, *Sol. Phys.*, 124, 145  
 Leroy, J. L. 1989, in *Dynamics and Structure of Quiescent Solar Prominences*, ed. E. R. Priest (Dordrecht: Kluwer), 102  
 Machado, M. E., Xiao, Y. C., Wu, S. T., Prokakis, T., & Dialetis, D. 1988, *ApJ*, 326, 425  
 Ramaty, R., & Murphy, R. J. 1987, *Space Sci. Rev.*, 45, 213  
 Rieger, E. 1989, *Sol. Phys.*, 121, 323  
 ———. 1991, in *IAU Colloq. 133, Eruptive Solar Flares*, ed. Z. Svestka, B. V. Jackson, & M. E. Machado (Lecture Notes in Physics 399) (Berlin: Springer), 161  
 Tang, F. 1985, *Sol. Phys.*, 102, 131  
 Wuelser, J. P., Canfield, R. C., & Rieger, E. 1990, in *Proc. MAX 91-Workshop No. 3*, ed. R. M. Winglee & A. L. Kiplinger (Boulder: Univ. Colorado Press), 149  
 Zaitsev, V. V., & Stepanov, A. V. 1983, *Sol. Phys.*, 88, 297